

Current Clinical Urology  
*Series Editor: Eric A. Klein*

Pat F. Fulgham  
Bruce R. Gilbert *Editors*

# Practical Urological Ultrasound

*Second Edition*

 Humana Press

# CURRENT CLINICAL UROLOGY

---

ERIC A. KLEIN, MD, SERIES EDITOR  
PROFESSOR OF SURGERY  
CLEVELAND CLINIC LERNER COLLEGE OF MEDICINE HEAD,  
SECTION OF UROLOGIC ONCOLOGY  
GLICKMAN UROLOGICAL AND KIDNEY INSTITUTE  
CLEVELAND, OH

---

Pat F. Fulgham • Bruce R. Gilbert  
Editors

# Practical Urological Ultrasound

Second Edition

 Humana Press

*Editors*

Pat F. Fulgham  
Department of Urology  
Texas Health Presbyterian Dallas  
Dallas, TX, USA

Bruce R. Gilbert  
Hofstra North Shore LIJ  
Smith Institute for Urology  
Great Neck, NY, USA

ISSN 2197-7194

ISSN 2197-7208 (electronic)

Current Clinical Urology

ISBN 978-3-319-43867-2

ISBN 978-3-319-43868-9 (eBook)

DOI 10.1007/978-3-319-43868-9

Library of Congress Control Number: 2016956231

© Springer International Publishing Switzerland 2017

This work is subject to copyright. All rights are reserved by the Publisher, whether the whole or part of the material is concerned, specifically the rights of translation, reprinting, reuse of illustrations, recitation, broadcasting, reproduction on microfilms or in any other physical way, and transmission or information storage and retrieval, electronic adaptation, computer software, or by similar or dissimilar methodology now known or hereafter developed.

The use of general descriptive names, registered names, trademarks, service marks, etc. in this publication does not imply, even in the absence of a specific statement, that such names are exempt from the relevant protective laws and regulations and therefore free for general use.

The publisher, the authors and the editors are safe to assume that the advice and information in this book are believed to be true and accurate at the date of publication. Neither the publisher nor the authors or the editors give a warranty, express or implied, with respect to the material contained herein or for any errors or omissions that may have been made.

Printed on acid-free paper

This Humana Press imprint is published by Springer Nature

The registered company is Springer International Publishing AG

The registered company address is: Gewerbestrasse 11, 6330 Cham, Switzerland

*To: Edwin Darracott Vaughan, M.D.  
(May 13, 1939–April 22, 2016), beloved mentor  
and friend who will always be an enduring inspiration.*

---

## Preface

The first edition of *Practical Urological Ultrasound* was an outgrowth of a campaign to teach practicing urologists the basic techniques for performing and documenting ultrasound examinations on urologic patients. An emphasis on an organ-based approach was intended to mimic what was encountered in daily practice and to extend the principles learned to intraoperative applications.

The more pervasive use of MRI in conjunction with radionuclide studies and, more recently, for MRI-guided prostate biopsy would seem to render a fundamental understanding of ultrasound less vital. To the contrary, the skillful use of ultrasound is critical to the co-registration of images for MRI-TRUS fusion biopsy of the prostate, for identification of lesions for focal therapy of the prostate, and for intraoperative guidance during complex renal surgery.

In fact, multi-parametric ultrasound (gray scale, Doppler, contrast-enhanced, and elastography) may function as well as MRI-based procedures in a variety of clinical situations at a fraction of the cost. In the short time since our first edition, improvements in transducers and overall image quality have made ultrasound a fundamental part of daily urologic practice and have the potential to replace axial imaging for some applications and procedures.

Central to urologist-performed imaging and imaging-based procedures is a thorough understanding of the physics underlying ultrasound imaging. We hope this edition will continue to enlighten urologists and encourage them to personally perform these procedures on behalf of their patients.

Dallas, TX, USA

Pat F. Fulgham

---

## Acknowledgments

The subject of this book has been a passion of mine for the past 10 years, and, like many roads in life, it would not have been possible without the support and tutelage of mentors, colleagues, and friends. I dedicate this book to the memory of Dr. E. Darracott Vaughan. He has always been my mentor and inspiration for the love of knowledge and teaching. In particular, for his vision, encouragement, and belief in me when I was a postgraduate research fellow in physiology, I owe my medical career to him.

This book was the vision of my coeditor, colleague, and friend Dr. Pat Fulgham. Through his leadership over these past years, he has helped elevate the art of urologic ultrasound to a subspecialty within urology. He is a gifted surgeon, articulate spokesman, and tireless academician who accepts nothing less than perfection from himself, which is contagious among all that have had the great fortune to work with him.

To the authors of this book, I am indebted. They have tirelessly given their precious time away from family and their busy clinical practices to share their experience. Their teachings as expressed in this text form the basis of urologic ultrasound.

My wife, and best friend, Betsy has been the most supportive and loving partner throughout the late nights and endless weekends involved in this project. She is, and has always been, my source of inspiration.

Bruce R. Gilbert

---

# Contents

|   |     |
|---|-----|
| <b>1 History of Ultrasound in Urology</b> .....   | 1   |
| Vinaya Vasudevan, Nikhil Waingankar, and Bruce R. Gilbert                               |     |
| <b>2 Physical Principles of Ultrasound</b> .....  | 13  |
| Pat F. Fulgham  |     |
| <b>3 Bioeffects and Safety</b> .....  | 31  |
| Pat F. Fulgham  |     |
| <b>4 Maximizing Image Quality: User-Dependent Variables</b> .....                       | 39  |
| Pat F. Fulgham  |     |
| <b>5 Renal Ultrasound</b> .....   | 51  |
| Daniel B. Rukstalis, Jennifer Simmons, and Pat F. Fulgham                               |     |
| <b>6 Scrotal Ultrasound</b> .....   | 77  |
| Etai Goldenberg, Gideon Richards, and Bruce R. Gilbert                                  |     |
| <b>7 Penile Ultrasound</b> .....  | 129 |
| Soroush Rais-Bahrami, Gideon Richards, and Bruce R. Gilbert                             |     |
| <b>8 Transabdominal Pelvic Ultrasound</b> .....   | 157 |
| R. Ernest Sosa and Pat F. Fulgham   |     |
| <b>9 Pelvic Floor Ultrasound</b> .....  | 169 |
| Ricardo Palmerola, Farzeen Firoozi, and Chad Baxter                                     |     |
| <b>10 Transrectal Ultrasound</b> .....  | 183 |
| Edouard J. Trabulsi, Xialong S. Liu, Whitney R. Smith,<br>and Akhil K. Das              |     |
| <b>11 Ultrasound for Prostate Biopsy</b> .....  | 197 |
| Christopher R. Porter and John S. Banerji   |     |
| <b>12 Pediatric Urologic Ultrasound</b> .....   | 211 |
| Lane S. Palmer and Adam Howe  |     |
| <b>13 Applications of Urologic Ultrasound During Pregnancy</b> .....                    | 229 |
| Majid Eshghi  |     |
| <b>14 Application of Urologic Ultrasound in Pelvic<br/>and Transplant Kidneys</b> ..... | 249 |
| Majid Eshghi  |     |

---

|   |     |
|---|-----|
| <b>15 Intraoperative Urologic Ultrasound</b> .....        | 267 |
| Fernando J. Kim and Rodrigo R. Pessoa                     |     |
| <b>16 Urologic Ultrasound Protocols</b> .....             | 287 |
| Bruce Gilbert   |     |
| <b>17 Urology Ultrasound Practice Accreditation</b> ..... | 341 |
| Nikhil Gupta and Bruce R. Gilbert                         |     |
| <b>Erratum to:</b> .....                                  | E1  |
| <b>Index</b> .....  | 351 |

---

## Contributors

**John Samuel Banerji, MD, MCh (Urology), DNB (Urology)** Section of Urology and Renal Transplantation, Virginia Mason, Seattle, WA, USA

**Z. Chad Baxter, M.D.** Department of Urology, UCLA David Geffen School of Medicine, Santa Monica, CA, USA

**Akhil Das, M.D.** Department of Urology, Sidney Kimmel Medical College at Thomas Jefferson University, Philadelphia, PA, USA

**Majid Eshghi, M.D., F.A.C.S., M.B.A.** Department of Urology, New York Medical College, Westchester Medical Center, New York, NY, USA

**Farzeen Firoozi, M.D., F.A.C.S.** Department of Urology, Hofstra Northshore–LIJ School of Medicine, The Arthur Smith Institute for Urology, Center of Pelvic Health and Reconstructive Surgery, Northwell Health System, Lake Success, NY, USA

**Pat Fox Fulgham, M.D., F.A.C.S.** Department of Urology, Texas Health Presbyterian Hospital of Dallas, Dallas, TX, USA

**Bruce R. Gilbert, M.D., Ph.D.** The Smith Institute for Urology, Northwell Health System, New Hyde Park, NY, USA

**Etai Goldenberg, M.D.** Urology Consultants, Ltd., Saint Louis, MO, USA

**Nikhil K. Gupta, M.D.** Smith Institute for Urology, Hofstra University, Northwell Health System, Lake Success, NY, USA

**Adam Howe, M.D.** Division of Pediatric Urology, Hofstra Northwell School of Medicine, Cohen Children’s Medical Center of New York of the Northwell Health System, Lake Success, NY, USA

**Fernando J. Kim, M.D., M.B.A., F.A.C.S.** Department of Urology, Denver Health Medical Center and University of Colorado Denver, Denver, CO, USA

**Xialong Shawn Liu, M.D.** Department of Urology, Tufts Medical Center, Boston, MA, USA

**Lane S. Palmer, M.D., F.A.C.S.** Division of Pediatric Urology, Hofstra Northwell School of Medicine, Cohen Children’s Medical Center of New York of the Northwell Health System, Lake Success, NY, USA

**Ricardo Palmerola, M.D.** Department of Urology, Hofstra Northshore–LIJ School of Medicine, The Arthur Smith Institute for Urology, Center of Pelvic Health and Reconstructive Surgery, Northwell Health System, Lake Success, NY, USA

**Rodrigo R. Pessoa, M.D.** Department of Urology, Denver Health Medical Center and University of Colorado Denver, Denver, CO, USA

**Christopher Robert Porter, M.D., F.A.C.S.** Section of Urology And Renal Transplantation, Virginia Mason, Seattle, WA, USA

**Soroush Rais-Bahrami, M.D.** Departments of Urology and Radiology, University of Alabama at Birmingham, Birmingham, AL, USA

**Gideon D. Richards, M.D.** Arizona State Urological Institute, Chandler, AZ, USA

**Daniel B. Rukstalis, M.D.** Department of Urology, Wake Forest Baptist Medical Center, Winston-Salem, NC, USA

**Jennifer Simmons, M.D.** Department of Urology, Geisinger Health System, Danville, PA, USA

**Whitney Smith, M.D.** Department of Urology, Sidney Kimmel Medical College at Thomas Jefferson University, Philadelphia, PA, USA

**R. Ernest Sosa, M.D.** Division of Urology, Veterans Administration Healthcare System, New York, NY, USA

**Edouard J. Trabulsi, M.D.** Department of Urology, Sidney Kimmel Medical College of Thomas Jefferson University, Philadelphia, PA, USA

**Vinaya Pavithra Vasudevan, M.D.** Smith Institute of Urology, Northwell Health Systems, New Hyde Park, NY, USA

**Nikhil Waingankar, M.D.** Department of Urology, Mt. Sinai Hospital, Astoria, NY, USA

Department of Population Health Science and Policy, Mt. Sinai Hospital, Astoria, NY, USA

Vinaya Vasudevan, Nikhil Waingankar,  
and Bruce R. Gilbert

## Introduction

Ultrasound is the portion of the acoustic spectrum characterized by sonic waves that emanate at frequencies greater than that of the upper limit of sound audible to humans, 20 kHz. A phenomenon of physics that is found throughout nature, ultrasound is utilized by rodents, dogs, moths, dolphins, whales, frogs, and bats for a variety of purposes, including communication, evading predators, and locating prey [1–4]. Lorenzo Spallanzani, an eighteenth century Italian Biologist and physiologist, was the first to provide experimental evidence that non-audible sound exists. Moreover, he hypothesized the utility of ultrasound in his work with bats

by demonstrating that bats use sound rather than sight to locate insects and avoid obstacles during flight; this was proven in an experiment where blind-folded bats were able to fly without navigational difficulty while bats with their mouths covered were not. He later determined through operant conditioning that the *Eptesicus fuscus* bat can perceive tones between 2.5 and 100 kHz [5, 6].

The human application of ultrasound began in 1880 with the work of brothers Pierre and Jacques Curie, who discovered that when pressure is applied to certain crystals, they generate electric voltage [7]. The following year, Gabriel Lippmann demonstrated the reciprocal effect that crystals placed in an electric field become compressed [8]. The Curies demonstrated that when placed in an alternating electric current, the crystals underwent either expansion or contraction and produced high frequency sound waves, thus creating the foundation for further work on piezoelectricity. Pierre Curie met his future wife Marie—with whom he later shared the Nobel Prize for their work on radioactivity [9]—in 1894 when Marie was searching for a way to measure the radioactive emission of uranium salts. She turned to the piezoelectric quartz crystal as a solution, combining it with an ionization chamber and quadrant electrometer; this marked the first time piezoelectricity was used as an investigative tool [10].

The sinking of the RMS Titanic in 1912 drove the public's desire for a device capable of echolocation, or the use of sound waves to locate hidden objects. This was intensified 2 years later with the

---

V. Vasudevan, M.D. (✉)  
Smith Institute of Urology, Northwell Health  
Systems, 450 Lakeville Road,  
New Hyde Park, NY 11042, USA  
E-mail: [vvasudevan@northwell.edu](mailto:vvasudevan@northwell.edu)

B.R. Gilbert, M.D., Ph.D.  
Hofstra Northwell School of Medicine, The Arthur  
Smith Institute for Urology, 450 Lakeville Road,  
Suite M41, New Hyde Park, NY 11042, USA  
E-mail: [bgilbert@gmail.com](mailto:bgilbert@gmail.com)

N. Waingankar, M.D.  
Department of Urology, Mt. Sinai Hospital,  
25-10 30th Ave, Astoria, NY 11102, USA

Department of Population Health Science and Policy,  
Mt. Sinai Hospital, 25-10 30th Ave,  
Astoria, NY 11102, USA  
E-mail: [WaingankarMD@gmail.com](mailto:WaingankarMD@gmail.com)

beginning of World War I, as submarine warfare became a vital part of both the Central and Allied Powers' strategies. Canadian inventor Reginald Aubrey Fessenden—perhaps most famous for his work in pioneering radio broadcasting and developing the Niagara Falls power plant—volunteered during World War I to help create an acoustic-based system for echolocation. Within 3 months he developed a high-power oscillator consisting of a 20 cm copper tube placed in a pattern of perpendicularly oriented magnetic fields that was capable of detecting an iceberg 2 miles away, and being detected underwater by a receiver placed 50 miles away [11].

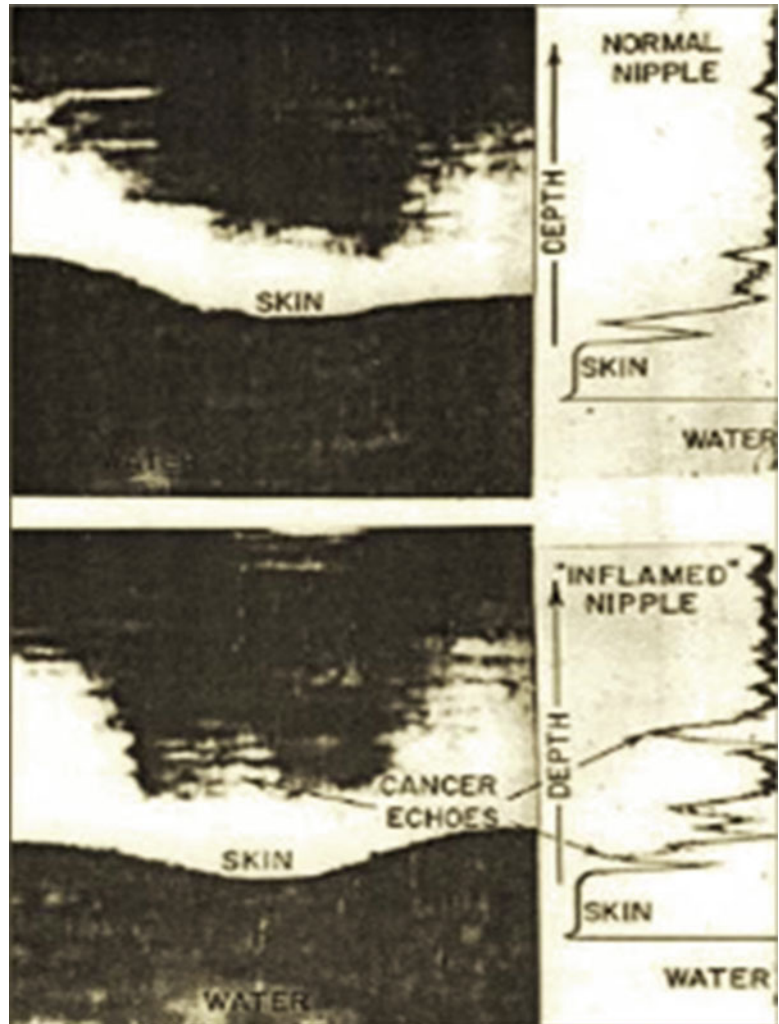
A contemporary of Fessenden and student of Pierre Curie, Paul Langevin was similarly interested in using acoustic technology for the detection of submarines in World War I. Using piezoelectricity, he developed an ultrasound generator in which the frequency of the alternating field was matched to the resonant frequency of the quartz crystals. This resonance evoked by the crystal produced mechanical waves that were transmitted through the surrounding medium in ultrasonic frequency, and were subsequently detected by the same crystals [12, 13]. Dubbed the “hydrophone,” this represented the first model of what we know today as sound navigation and ranging, or SONAR. Although there were only sporadic reports on the use of SONAR in sinking German U-boats, SONAR was vital to both the Allied and Axis Powers during World War II [14].

In 1928, Russian scientist Sergei Sokolov further advanced the applicability of ultrasound in his experiments at Ulyanov Electrotechnical Institute. Using a “reflectoscope,” Sokolov directed sound waves through metal objects, which were reflected at the opposite side of the object and traveled back to the reflectoscope. He determined that flaws within the metals would alter the otherwise predictable course of the sound waves. Sokolov also proposed the first “sonic camera,” in which a metal's flaw could be imaged in high resolution. The actual output, however, was not adequate for practical usage. These early experiments describe what we now know as through transmission [15]. Sokolov is regarded by many as the “Father of Ultrasonics,” and was awarded the Stalin prize for his work [13].

In 1936, German scientist Raimar Pohlman described an ultrasonic imaging method based on transmission via acoustic lenses, with conversion of the acoustic image into a visual entity. Two years later, Pohlman became the first to describe the use of ultrasound as a treatment modality when he observed its therapeutic effect when introduced into human tissues [16]. Austrian neurologist Karl Dussik is credited with being the first to use ultrasound as a diagnostic tool. In 1940 in a series of experiments attempting to map the human brain and potentially locate brain tumors, transducers were placed on each side of a patient's head, which along with the transducers, was partially immersed in water. At a frequency of 1.2 MHz, Dussik's “hyperphonography” was able to produce low resolution “ventriculograms” [17]. Other investigators were unable to reproduce the same images as Dussik, sparking controversy that this may have not been true images of the cerebral ventricles, but rather, acoustic artifact. Dussik's work led MIT physician HT Ballantyne to conduct similar experiments, where they demonstrated that an empty skull produces the same images obtained by Dussik. They concluded that attenuation patterns produced by the skull were contributing to the patterns that Dussik had previously thought resulted from changes in acoustic transmission caused by the ventricles. These findings led the United States Atomic Energy Commission to conclude that ultrasound had no role in the diagnosis of brain pathology [18, 19].

In 1949, John Wild, a surgeon who had spent time in World War II treating numerous soldiers with abdominal distention following explosions, used military aviation-grade ultrasonic equipment to measure bowel thickness as a noninvasive tool to determine the need for surgical intervention. He later used A-mode comparisons of normal and cancerous tissue to demonstrate that ultrasound could be useful in the detection of cancer growth. Wild teamed up with engineer John Reid to build the first portable “echograph” for use in hospitals (see Fig. 1.1) and also to develop a scanner that was capable of detecting breast and colon cancer by using pulsed waves to allow display the location and reflectivity of an object, a mode that would later be described as “brightness mode,” or simply B-mode [13, 20, 21].

**Fig. 1.1** An example of one of Wild and Reid's original echographs, pictured above, was used to measure skin thickness as compared to breast cancer tissue thickness to determine a diagnosis of breast cancer [22]. *Reproduced with permission from Hill CR, Early days of scanning: Pioneers and Sleepwalkers, in Radiography. 2009 (15): p. 15–22, courtesy of Elsevier*



Following the post-World War II resurgence of interest in cardiac surgery, Inge Edler and Hellmuth Hertz began to investigate noninvasive methods of detecting mitral stenosis, a disease with relatively poor results at the time. Using an ultrasonic reflectoscope with tracings recorded on slowly moving photographic film designed by Hertz (see Fig. 1.2), they were able to capture moving structures within the heart. Dubbed “Ultrasound Cardiology,” this represented the first echocardiogram, which was capable of differentiating mitral stenosis from mitral regurgitation, and detecting atrial thrombi, myxomas, and pericardial effusions [23, 24].

With the support of the Veterans Administration and United States Public Health Service, Holmes

et al. described the use of ultrasound to detect soft tissue structures with an ultrasonic “sonascope.” This consisted of a large water bath in which the patient would sit, a sound generator mounted on the tub, and an oscilloscope which would display the images. The sonascope was capable of identifying a cirrhotic liver, renal cyst, and differentiating veins, arteries, and nerves in the neck. Consistent with the results of their predecessors, however.

The use of ultrasound in obstetrics and gynecology began in 1954 when Ian Donald became interested in the use of A-mode, or amplitude-mode, which uses a single transducer to plot echoes on a screen as a function of depth; one of the early uses of this was to differentiate solid from cystic masses.

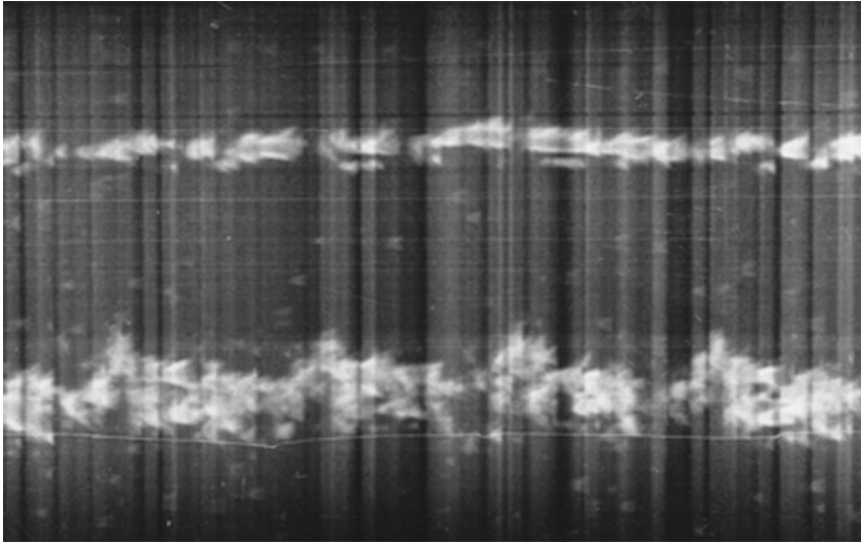


**Fig. 1.2** The first echocardiographic recording is displayed as a “motion-mode,” or M-mode, tracing displaying ultrasonic tracings of the left ventricular posterior wall [24]. Reproduced with permission from Fraser, A.G., Inge

*Edler and the origins of clinical echocardiography. Eur J Echocardiogr, 2001. 2(1): p. 3–5, courtesy of Oxford University Press*

Using a borrowed flaw-detector, he initially found that the patterns of the two masses were sonically unique. Working with the research department of an atomic boilermaker company, he led a team that developed the first contact scanner. Obviating the need for a large water bath, this device was hand-operated and kept in contact with skin and coupled with olive oil. Captured on Polaroid® film with an open shutter, abdominal masses could be reliably and reproducibly differentiated using ultrasound. Three years later, Donald collaborated with his team of engineers to develop a means to measure distances on the output on a cathode ray tube, which was subsequently used to determine fetal head size [13, 25–27].

## History of Doppler Ultrasound

In 1842, Christian Johann Doppler theorized that the frequency of light received at a distance from a fixed source is different than the frequency emitted if the source is in motion [28]. More than 100 years later, this principle was applied to sound by Satomura in his study on cardiac valvular motion and peripheral blood vessel pulsation [29]. In 1958, Seattle pediatri-

cian Rushmer and his team of engineers further advanced the technology with their development of transcutaneous continuous-wave flow measurements and spectral analysis in peripheral and extracranial brain vessels [30]. Real-time imaging—developed in 1962 by Homes—was born out of the principal of “compounding,” which allowed the sonographer to sweep the transducer across the target to continuously add information to the scan; the phosphor-decay display left residual images from the prior transducer position on the screen, allowing the entire target to be visualized [13]. The first commercially available real-time scanner was produced by Siemens, and its first published use was in the diagnosis of hydrops fetalis [31, 32].

Bernstine and Callagan were the first to report the obstetric utility of Doppler in their 1964 report on ultrasonic detection of fetal heart movement, thus laying the foundation for continuous fetal monitoring [33]. The same year, Buschmann was the first report “carotid echography” for the diagnosis of carotid artery thrombosis [34], although debate ensued as to whether ultrasound was capable of identifying the carotid bifurcation or its branches into the internal and external carotid arteries [35–37].

In 1966, Kato and Izumi developed directional Doppler that was capable of determining direction of flow [32, 38]. The following year, McLeod reported similar findings using phase shift in the United States [30, 39, 40]. By 1967, the use of Doppler ultrasound had spread to Europe, where continuous-wave ultrasound (which does not allow precise spatial localization) was being used to diagnose occlusive disease of neck and limb arteries, venous thrombosis, and valvular insufficiency with accuracy [41]. Pulsed Doppler soon provided the capability of sampling specific Doppler signals in target tissues, a function that quickly became clinically applicable in the detection of valvular motion and differential flow rates within the heart [42].

The addition of color flow mapping to Doppler ultrasound allowed real-time mapping of blood flow patterns [43]. The limitations of color flow, including angle dependence and difficulty assessing flow in slow-flow states, were soon appreciated. These were overcome with the advent of an alternative form of Doppler, termed “Power Doppler.” This alternative to routine color flow was found to be useful in confirming or excluding difficult cases of testicular or ovarian torsion and vascular thrombosis [44].

Researchers next turned their attention to techniques to improve the clarity and reduce artifact within ultrasound-guided images. In 1980, real-time compound sonography was developed by using the probe to obtain multiple images from

different viewing angles. Computed beam steering technology is then used to combine multiplanar images into one compound image in real time. Summation of these images reduced artifact and improved delineation of surfaces. This technique was expanded from linear array to curved array transducers, making it more accessible for abdominal and pelvic imaging. Now, compound sonography is used for musculoskeletal, vascular, hepatobiliary, and pelvic imaging [45].

In 1989, Baba and colleagues reported on the first production of a three-dimensional ultrasonic image. Using a real-time straight or curved transducer, they were able to obtain positional information with an ultrasound device that was connected to a microcomputer, which reconstructed the data into a three-dimensional output. The authors hypothesized that this system would be ideal for the screening of fetal anomalies and abnormalities in intrauterine growth [44]. Following the development of von Ramm’s three-dimensional ultrasound device, Sheikh et al. published the first use of real-time three-dimensional acquisition and presentation of data in the United States in 1991. This proved to be useful in cardiology for assessment of perfusion and ventricular function [46].

In 1996, several authors including Burns et al. began exploring the realm of tissue harmonic sonography (see Fig. 1.3) as a means to overcome image degradation [45, 47]. During the initial investigation, the authors explored microbubble

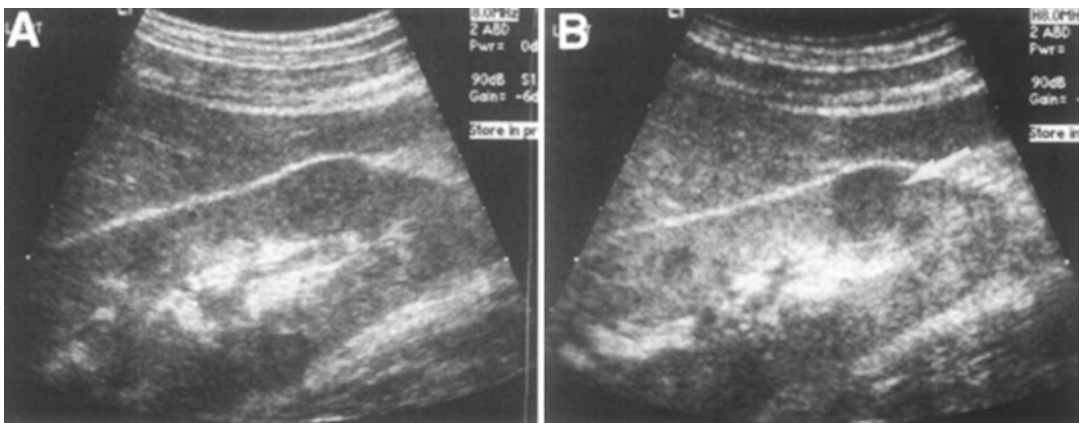


**Fig. 1.3** Here, a fundamental mode image of the kidney reveals a focal contour of an abnormality seen in the lower pole, while the harmonic mode image, to the right, reveals that the lesion is solid in nature [47]. *Reproduced with*

*permission from Dessler, T.S., et al., Tissue Harmonic Imaging Techniques: Physical Principles and Clinical Applications. Seminars in Ultrasound, CT, and MRI. 2001. 22(1): 1–10, courtesy of Elsevier*

ultrasound contrast media to improve contrast agent-specific images, with the result that the harmonic signal was stronger from the microbubbles than the signal from tissue. Now, harmonic mode has developed as a gray scale ultrasound mode that employs echoes at twice the transmitted frequency. This technique has resulted in improved image clarity and decreased artifact, and has proven invaluable in diagnosis of pathology in the hepatobiliary tree and genitourinary tract, most importantly in determining distinguishing characteristics of cystic and solid lesions.

Electronic steering of the ultrasound beam is the process of using parallel beams oriented along multiple directions from an array transducer along different directions. This is also referred to as multibeam imaging. The arrays obtained from each direction are compounded into a single image, which increases the lateral resolution and reduces the noise levels [48].

## History of Ultrasound in Urology

### Prostate

In 1963, Japanese Urologists Takahashi and Ouchi became the first to attempt ultrasonic examination of the prostate. However, the image quality that resulted was not interpretable and thus carried little medical utility [49]. Wild and Reid also attempted transrectal ultrasound, but were met with the same result. Progress was not made until Watanabe et al. demonstrated radial scanning that could adequately identify prostate and bladder pathology. Using a purpose-built device modeled after a museum sculpture entitled “Magician’s Chair,” Watanabe seated his patients on a chair with a hole cut in the center such that the transducer tube could be passed through the hole and into the rectum of the seated patient [50]. Images from Watanabe’s seated probe are displayed in Fig. 1.4a; it is evident in Fig. 1.4b

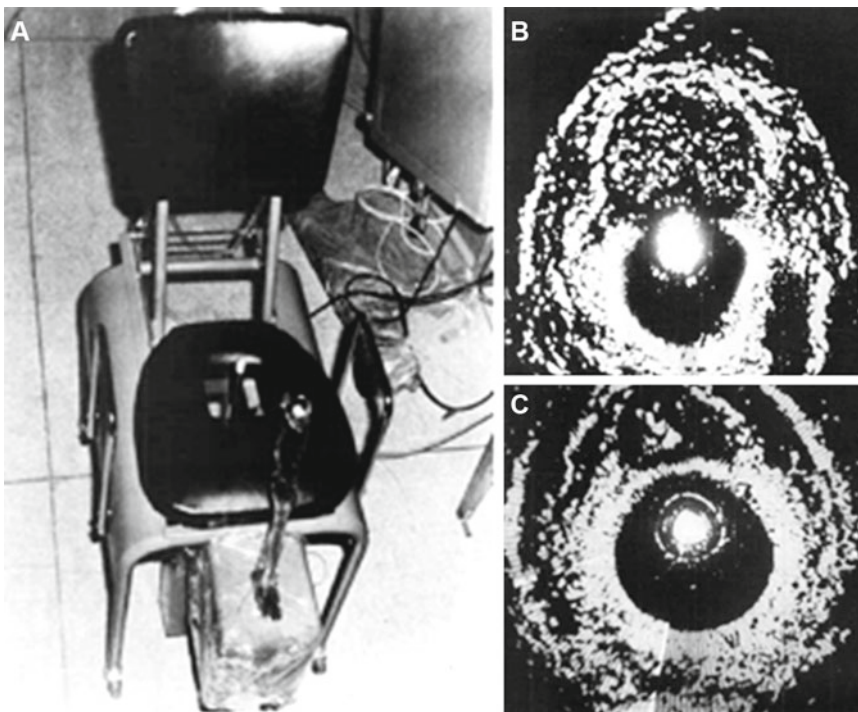


**Fig. 1.4** (a) Images from Watanabe’s seated probe are displayed [50], revealing (b) an area of circumscribed symmetric echogenicity, representing BPH, (c) an asymmetric area of hyperechogenicity, representing prostate cancer. In these images, note that resolution was poor, and

images displayed extreme contrast. *Reproduced with permission from Watanabe, H., et al., Development and application of new equipment for transrectal ultrasonography. J Clin Ultrasound, 1974. 2(2): p. 91–8, courtesy of John Wiley and Sons*

(demonstrating an area of circumscribed symmetric echogenicity, representing BPH) and Fig. 1.4c (demonstrating an asymmetric area of hyperechogenicity, representing prostate cancer) that resolution was poor and images displayed extreme contrast. Subsequent development of biplane, high frequency probes has created increased resolution and has allowed for transrectal ultrasound to become the standard for diagnosis of prostatic disease.

In 1974, Holm and Northeved introduced a transurethral ultrasonic device that would be interchangeable with conventional optics during cystoscopy for the purpose of imaging the prostate and bladder. Their other goals for this device included the ability to determine depth of bladder tumor penetration, prostatic volume, evaluation of prostatic tumor progression, and to assist with transurethral resection of prostate [51].

More recently, several other techniques have come to light in the diagnosis of prostate cancer.

The concept of multiparametric MRI, in which MRI images are electronically superimposed in real time on transrectal ultrasound (see Fig. 1.5), has further revolutionized the ability to detect high-risk prostate cancer [52].

Histoscanning has also been used to more accurately define prostatic lesions. This involves three steps: a motorized transrectal ultrasound, a software analysis to define the region of concern, and a color-coded analysis of tissue detailing all region suspicion [54].

Finally, sonoelastography, a technique for assessing tissue elasticity to distinguish cancer tissue from prostate parenchyma, has been shown to improve detection rates when ultrasound-guided biopsies alone are insufficient to define the target

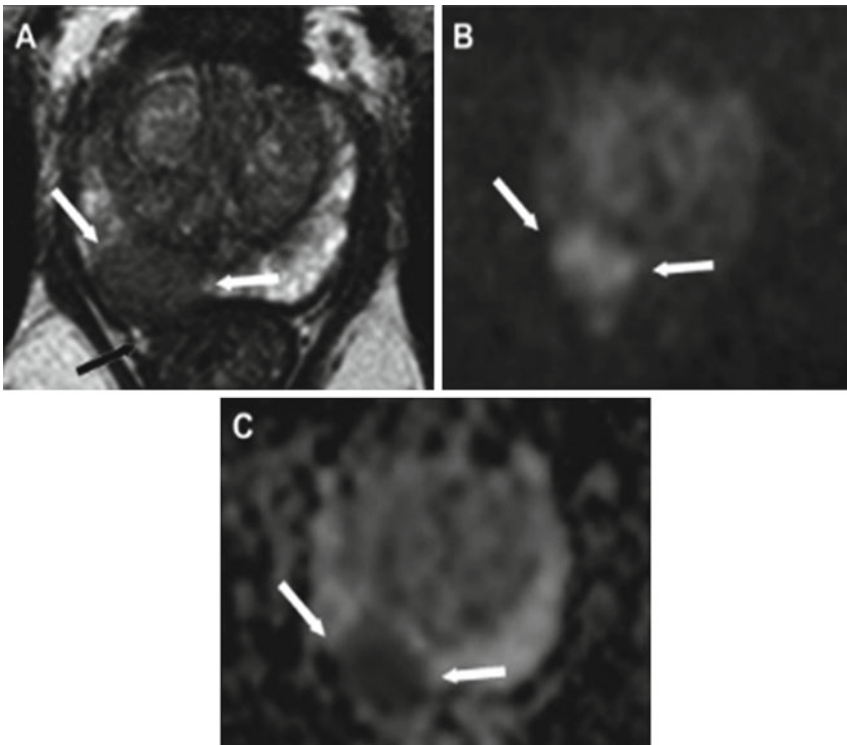


**Fig. 1.5** In this example, a multiparametric MRI, T2 weighted, was obtained and outlines a suspicious lesion. (a) A hypointense lesion in the right peripheral zone of the prostate is noted with extracapsular extension. The lesion is hyperintense on DWI imaging. (b) A TRUS-guided biopsy, performed with the ADC map shown here (c),

revealed Gleason grade 9 (4+5) disease in this patient [53]. *Reproduced with permission from Oliveira Neto JA, Parente DB. Multiparametric Magnetic Resonance Imaging of the Prostate. Magnetic Resonance Imaging Clinics of North America. 2013 (21): p. 409–26, courtesy of Elsevier*

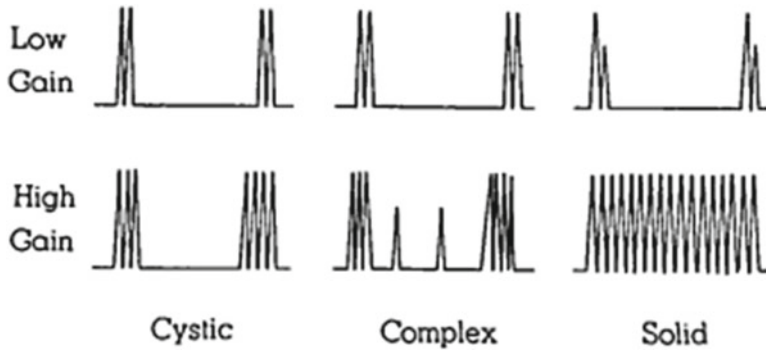


**Fig. 1.6** This is a diagrammatic representation of the three types of ultrasound patterns obtained from masses. In this way, ultrasound has been able to distinguish the differences between the solid, cystic, and necrotic masses

(a mixture of solid and cystic masses) [57]. *Reproduced with permission from Goldberg, B.B. and H.M. Pollack, Differentiation of renal masses using A-mode ultrasound. J Urol, 1971. 105(6): p. 765–71, courtesy of Elsevier*

[55]. A sensitivity of 0.81, specificity of 0.69, and accuracy of 0.74 for detection of prostate cancer were found by Boehm et al. [56], which is similar to that of MRI.

## Kidney

In 1971, Goldberg and Pollack, frustrated with the inability of IVP to differentiate benign from malignant lesions, turned to A-mode ultrasound. In their report on “nephrosonography,” they demonstrated in a series of 150 patients the capability of ultrasound to discern solid, cystic, and complex masses with an accuracy of 96%. The diagrammatic representation of the three ultrasound patterns they found is depicted in Fig. 1.6 [57]. In cystic lesions, the first spike represents the striking of the front wall of the cyst and the second spike represents the striking of the back wall. More complex lesions therefore have return of more spikes.

## Scrotum

Perri et al. were the first to use Doppler as a sonic “stethoscope” in their workup of patients with an acute scrotum. While they were able to

identify patients with epididymitis and torsion of the appendix testis as having increased flow, and patients with spermatic cord torsion as having no blood flow, they also reported that false negatives in cases of torsion could result from increased flow secondary to reactive hyperemia [58, 59].

## Further Advancements

Watanabe and colleagues demonstrated that Doppler could be used to identify the renal arteries in a noninvasive way in 1976 [60], and 5 years afterward, Greene and colleagues documented that Doppler could adequately differentiate stenotic from normal renal arteries [61]. In 1982, Arima et al. used Doppler to differentiate acute from chronic rejection in renal transplant patients, noting that acute rejection is characterized by the disappearance of diastolic phase, with reappearance being indicative of recovery from rejection. The authors concluded that Doppler could guide the management of rejection as an index for steroid therapy [62].

In the early 1990s, a number of authors investigated the therapeutic uses of high-intensity focused ultrasound, or HIFU. Following prior reports of histologic changes following HIFU [63], Marberger and colleagues were the first to

report the safety and efficacy of HIFU in symptomatic BPH patients [64]. Its utilities in the treatments of testicular cancer [65], early prostate cancer [66], recurrent prostate cancer [67], and renal cell cancer (transcutaneously [68] and laparoscopically [69]) were soon explored as well.

The field of urology continues to demand and discover novel uses for ultrasound technology. Chen et al. used transrectal ultrasound guidance to inject botulinum toxin into the external urethral sphincters of a series of patients with detrusor external sphincter dyssynergia [70]. Ozawa and colleagues used perineal ultrasound videourodynamics to accurately diagnose bladder outlet obstruction in a new, noninvasive method [71]. The possibilities for the application of ultrasound in diagnosing or treating urologic patients remain endless.

### Conclusion

Ultrasound is a cost-effective, accurate, and nearly ubiquitous easy to use diagnostic tool that produces meaningful results instantly. As a standard in the urologist’s office armamentarium, it can be applied to the workup of pathology of the genitalia, pelvic floor, bladder, prostate, and kidneys. Specific uses within each organ system will be detailed throughout this book.

The history of ultrasound is quite extensive and has involved a number of groundbreaking discoveries and new applications of basic physical principles (see Fig. 1.7). In the future, multiparametric imaging and multidimensional real-time ultrasound will allow for enhanced diagnostic and therapeutic utility of ultrasound in multiple different clinical settings. This homage to the innovators of the past serves both to recognize prior achievements and to acknowledge that future work in the development of new applications for ultrasound will always be needed.

## A History of Ultrasound

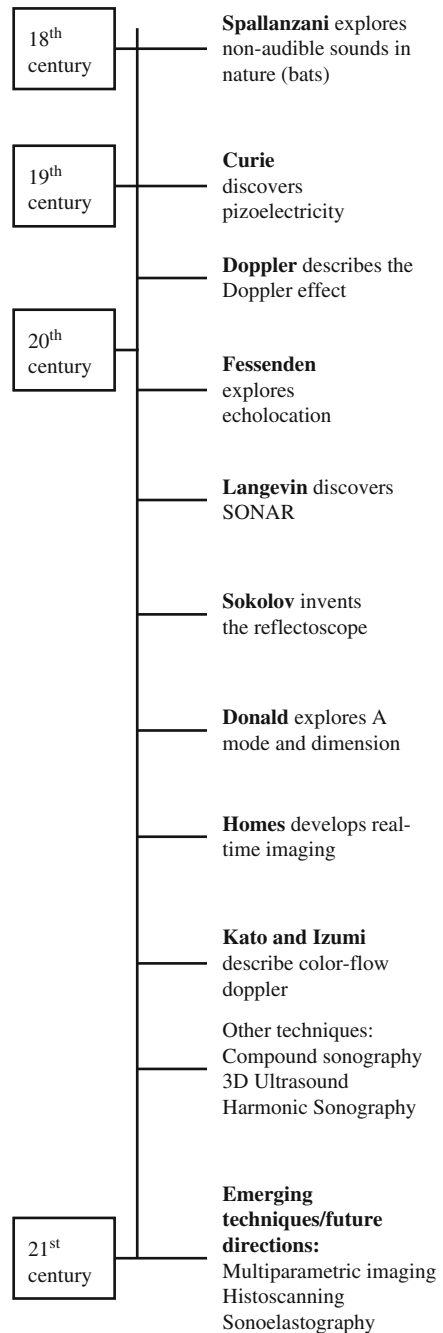


**Fig. 1.7** A timeline detailing the history of important contributions to the field of ultrasonography

## References

- Corcoran AJ, Barber JR, Conner WE. Tiger moth jams bat sonar. *Science*. 2009;325(5938):325–7.
- Dunning DR, Roeder KD. Moth sounds and the insect-catching behavior of bats. *Science*. 1965;147:173–4.
- Mackay RL, Liaw HM. Dolphin vocalization mechanisms. *Science*. 1981;212(4495):676–8.
- Ruttimann J. Frogs chat in ultrasound. *Nature News*. 2006.
- Galambos R. The avoidance of obstacles by flying bats: Spallanzani's ideas (1794) and later theories. *Isis*. 1942;34(2):132–40.
- Dijkgraaf S. Spallanzani's unpublished experiments on the sensory basis of object perception in bats. *Isis*. 1960;51(1):9–20.
- Curie J, Curie P. Sur l'électricité polaire dans cristaux hémédres a face inclinées. *C R Seances Acad Sci*. 1880;91:383.
- Katzir S. The discovery of the piezoelectric effect. In: *The beginnings of piezoelectricity: a study in mundane physics*. Netherlands: Springer; 2006. p. 15–64.
- Curie P. Radioactive substances, especially radium. In: *Nobel Lecture*. 1905.
- Diamantis A, Magiorkinis E, Papadimitriou A, Androustos G. The contribution of Maria Skłodowska-Curie and Pierre Curie to nuclear and medical physics. A hundred and ten years after the discovery of radium. *Hell J Nucl Med*. 2008;11(1):33–8.
- Seitz F. The cosmic inventor: Reginald Aubrey Fessenden (1866–1932). *Am Philos Soc*. 1999;89:41–6.
- Chilowsky C, Langevin M. Procédés et appareils pour la production de signaux sous-marins dirigés et pour la localisation a distance d'obstacles sous-marins. 1916.
- Martin J. History of ultrasound. In: Sanders R, Resnick M, editors. *Ultrasound in urology*. Baltimore: Williams and Wilkins; 1984. p. 1–12.
- Zimmerman D. Paul Langevin and the discovery of active sonar or asdic. *North Mar*. 2002;12(1):39–52.
- Sokolov SY. The ultra-acoustic microscope. *Zh Tekh Fiz*. 1949;19:271.
- Jagannathan J, et al. High-intensity focused ultrasound surgery of the brain: part 1—a historical perspective with modern applications. *Neurosurgery*. 2009;64(2):201–10. discussion 210–1.
- Dussik K. Über die Möglichkeit, hochfrequente mechanische Schwingungen als diagnostische Mittel zu verwerten. *Z Ges Neurol Psych*. 1941;174:153–68.
- Thomas AMK, Banerjee A, Busch U. Über die Möglichkeit, hochfrequente mechanische Schwingungen als diagnostische Mittel zu verwerten. In: Banerjee A, Thomas AMK, Busch U, editors. *Classic papers in modern diagnostic radiology*. Berlin: Springer; 2005. p. 144–61.
- Shampo MA, Kyle RA. Karl Theodore Dussik—pioneer in ultrasound. *Mayo Clin Proc*. 1995;70(12):1136.
- Thomas AMK, Banerjee A, Busch U. Application of echo-ranging techniques to the determination of structure of biological tissues. In: Banerjee A, Thomas AMK, Busch U, editors. *Classic papers in modern diagnostic radiology*. Berlin: Springer; 2005. p. 162–9.
- Wild JJ, Reid JM. Application of echo-ranging techniques to the determination of structure of biological tissues. *Science*. 1952;115(2983):226–30.
- Hill CR. Early days of scanning: pioneers and sleepwalkers. *Radiography*. 2009;15:15–22.
- Edler I, Hertz CH. The use of ultrasonic reflectoscope for the continuous recording of the movements of heart walls. *Clin Physiol Funct Imaging*. 2004;24(3):118–36.
- Fraser AG. Inge Edler and the origins of clinical echocardiography. *Eur J Echocardiogr*. 2001;2(1):3–5.
- Holmes JH, et al. The ultrasonic visualization of soft tissue structures in the human body. *Trans Am Clin Climatol Assoc*. 1954;66:208–25.
- Donald I, Macvicar J, Brown TG. Investigation of abdominal masses by pulsed ultrasound. *Lancet*. 1958;1(7032):1188–95.
- Thomas AMK, Banerjee AK, Busch U. Investigation of abdominal masses by pulsed ultrasound. In: Thomas AMK, Banerjee AK, Busch U, editors. *Classic papers in modern diagnostic radiology*. Berlin: Springer; 2005. p. 213–23.
- Doppler C. Über das farbige Licht der Doppelsterne und einiger anderer Gestirne des Himmels. *Abh Königl Böhm Ges Wiss*. 1843;2:465–82.
- Satomura S. Ultrasonic Doppler method for the inspection of cardiac function. *J Acoust Soc Am*. 1957;29:1181–5.
- Coman IM. Christian Andreas Doppler—the man and his legacy. *Eur J Echocardiogr*. 2005;6(1):7–10.
- Hofmann D, Hollander HJ. Intrauterine diagnosis of hydrops fetus universalis using ultrasound. *Zentralbl Gynakol*. 1968;90(19):667–9.
- Woo J. A short history of the development of ultrasound in obstetrics and gynecology. [http://www.ob-ultrasound.net/site\\_index.html](http://www.ob-ultrasound.net/site_index.html).
- Bernstine RL, Callagan DA. Ultrasonic Doppler inspection of the fetal heart. *Am J Obstet Gynecol*. 1966;95(7):1001–4.
- Buschmann W. On the diagnosis of carotid thrombosis. *Albrecht Von Graefes Arch Ophthalmol*. 1964;166:519–29.
- Brinker RA, Landiss DJ, Croley TF. Detection of carotid artery bifurcation stenosis by Doppler ultrasound. Preliminary report. *J Neurosurg*. 1968;29(2):143–8.
- Grossman BL, Wood EH. Evaluation of cerebrovascular disease utilizing a transcutaneous Doppler technique. *Radiology*. 1968;90(3):586–7.
- Strandness Jr. D. Ultrasonic velocity determination in the diagnosis and evaluation of peripheral vascular disease. In: *Symposium on ultrasound*. Indiana University; 1968.
- Kato K, Izumi T. A new ultrasonic flowmeter that can detect flow direction. In: *Proceedings of the tenth scientific meeting of the Japan Society of Ultrasonics in Medicine*; 1966. p. 78–9.
- Maroon JC, Campbell RL, Dyken ML. Internal carotid artery occlusion diagnosed by Doppler ultrasound. *Stroke*. 1970;1(2):122–7.

40. McLeod F. A directional Doppler flowmeter. In: Digest of the seventh international conference on medical electronics and biological engineering; 1967. p. 213.
41. Bollinger A, Partsch H. Christian Doppler is 200 years young. *Vasa*. 2003;32(4):225–33.
42. Baker DW, Johnson SL, et al. Doppler echocardiography. In: Waag R, Gramiak R, editors. *Cardiac ultrasound*. St. Louis: CV Mosby; 1974. p. 24.
43. Maulik D, et al. Doppler color flow mapping of the fetal heart. *Angiology*. 1986;37(9):628–32.
44. Hamper UM, et al. Power Doppler imaging: clinical experience and correlation with color Doppler US and other imaging modalities. *Radiographics*. 1997;17(2):499–513.
45. Oktar SO, et al. Comparison of conventional sonography, real-time compound sonography, tissue harmonic sonography, and tissue harmonic compound sonography of abdominal and pelvic lesions. *AJR*. 2003;181:1341–7.
46. Sheikh K, et al. Real-time, three-dimensional echocardiography: feasibility and initial use. *Echocardiography*. 1991;8(1):119–25.
47. Desser TS, et al. Tissue harmonic imaging techniques: physical principles and clinical applications. *Semin Ultrasound CT MR*. 2001;22(1):1–10.
48. Chan V, et al. Basics of ultrasound imaging. In: *Atlas of ultrasound-guided procedures in interventional pain management*, vol. 1. New York: Springer; 2011. p. 13–9.
49. Takahashi H, Ouchi T. The ultrasonic diagnosis in the field of urology. *Proc Jpn Soc Ultrason Med*. 1963;3:7.
50. Watanabe H, et al. Development and application of new equipment for transrectal ultrasonography. *J Clin Ultrasound*. 1974;2(2):91–8.
51. Holm HH, Northeved A. A transurethral ultrasonic scanner. *J Urol*. 1974;111(2):238–41.
52. Siddiqui M, Rais-Bahrami S, Turkbey B, et al. Comparison of MR/ultrasound fusion-guided biopsy with ultrasound-guided biopsy for the diagnosis of prostate cancer. *JAMA*. 2015;313(4):390–7.
53. Oliveira Neto JA, Parente DB. Multiparametric magnetic resonance imaging of the prostate. *Magn Reson Imaging Clin N Am*. 2013;21:409–26.
54. Koh J, et al. Additional targeted biopsy in clinically suspected prostate cancer: prospective randomized comparison between contrast-enhanced ultrasound and sonoelastography guidance. *Ultrasound Med Biol*. 2015;41(11):2836–41.
55. Yen C-L, et al. The benefits of comparing conventional sonography, real-time spatial compound sonography, tissue harmonic sonography, and tissue harmonic compound sonography of hepatic lesions. *Clin Imaging*. 2008;32:11–5.
56. Boehm K, Salomon G, Beyer B, Schiffmann J, Simonis K, Graefen M, Budaes L. Shear wave elastography for localization of prostate cancer lesions and assessment of elasticity thresholds: implications for targeted biopsies and active surveillance protocols. *J Urol*. 2015;2014(193):794–800.
57. Goldberg BB, Pollack HM. Differentiation of renal masses using A-mode ultrasound. *J Urol*. 1971;105(6):765–71.
58. Perri AJ, et al. Necrotic testicle with increased blood flow on Doppler ultrasonic examination. *Urology*. 1976;8(3):265–7.
59. Perri AJ, et al. The Doppler stethoscope and the diagnosis of the acute scrotum. *J Urol*. 1976;116(5):598–600.
60. Watanabe H, et al. Non-invasive detection of ultrasonic Doppler signals from renal vessels. *Tohoku J Exp Med*. 1976;118(4):393–4.
61. Greene ER, et al. Noninvasive characterization of renal artery blood flow. *Kidney Int*. 1981;20(4):523–9.
62. Arima M, et al. Predictability of renal allograft prognosis during rejection crisis by ultrasonic Doppler flow technique. *Urology*. 1982;19(4):389–94.
63. Burgess SE, et al. Histologic changes in porcine eyes treated with high-intensity focused ultrasound. *Ann Ophthalmol*. 1987;19(4):133–8.
64. Madersbacher S, et al. Tissue ablation in benign prostatic hyperplasia with high-intensity focused ultrasound. *Eur Urol*. 1993;23 Suppl 1:39–43.
65. Madersbacher S, et al. Transcutaneous high-intensity focused ultrasound and irradiation: an organ-preserving treatment of cancer in a solitary testis. *Eur Urol*. 1998;33(2):195–201.
66. Chapelon JY, et al. Treatment of localised prostate cancer with transrectal high intensity focused ultrasound. *Eur J Ultrasound*. 1999;9(1):31–8.
67. Berge V, Baco E, Karlsen SJ. A prospective study of salvage high-intensity focused ultrasound for locally radiorecurrent prostate cancer: Early results. *Scand J Urol Nephrol*. 2010;44(4):223–7.
68. Kohrman KU, et al. High intensity focused ultrasound as noninvasive therapy for multilocal renal cell carcinoma: case study and review of the literature. *J Urol*. 2002;167(6):2397–403.
69. Margreiter M, Marberger M. Focal therapy and imaging in prostate and kidney cancer: high-intensity focused ultrasound ablation of small renal tumors. *J Endourol*. 2010;24(5):745–8.
70. Chen SL. Transrectal ultrasound-guided transperineal botulinum toxin a injection to the external urethral sphincter for treatment of detrusor external sphincter dyssynergia in patients with spinal cord injury. *Arch Phys Med Rehabil*. 2010;91(3):340–4.
71. Ozawa H, et al. The future of urodynamics: non-invasive ultrasound videourodynamics. *Int J Urol*. 2010;17(3):241–9.

Pat F. Fulgham

---

## Introduction

The use of ultrasound is fundamental to the practice of urology. In order for urologists to best use this technology on behalf of their patients, they must have a thorough understanding of the physical principles of ultrasound. Understanding how to tune the equipment and to manipulate the transducer to achieve the best-quality image is crucial to the effective use of ultrasound. The technical skills required to perform and interpret urologic ultrasound represent a combination of practical scanning ability and knowledge of the underlying disease processes of the organs being imaged. Urologists must understand how ultrasound affects biological tissues in order to use this modality safely and appropriately. When the physical principles of ultrasound are fully understood, urologists will recognize both the advantages and limitations of ultrasound.

---

The original version of this chapter was revised.  
An erratum to this chapter can be found at  
DOI [10.1007/978-3-319-43868-9\\_18](https://doi.org/10.1007/978-3-319-43868-9_18)

P.F. Fulgham, M.D., F.A.C.S. (✉)  
Department of Urology, Texas Health Presbyterian  
Dallas, 8210 Walnut Hill Lane Suite 014,  
Dallas, TX 75231, USA  
e-mail: [pfulgham@airmail.net](mailto:pfulgham@airmail.net)

---

## The Mechanics of Ultrasound Waves

The image produced by ultrasound is the result of the interaction of mechanical ultrasound waves with biologic tissues and materials. Because ultrasound waves are transmitted at frequent intervals and the reflected waves received by the transducer, the images can be reconstructed and refreshed rapidly, providing a real-time image of the organs being evaluated. Ultrasound waves are **mechanical waves** which require a physical medium (such as tissue or fluid) to be transmitted. Medical ultrasound imaging utilizes frequencies in the one million cycles per second (or MHz) range. Most transducers used in urology vary from 2.5 to 18 MHz, depending on the application.

Ultrasound waves are created by applying alternating current to piezoelectric crystals within the transducer. Alternating expansion and contraction of the piezoelectric crystals creates a mechanical wave which is transmitted through a coupling medium (usually gel) to the skin and then into the body. The waves that are produced are **longitudinal waves**. This means that the particle motion is in the same direction as the propagation of the wave (Fig. 2.1). This longitudinal wave produces areas of rarefaction and compression of tissue in the direction of travel of the ultrasound wave.

The compression and rarefaction of molecules is represented graphically as a sine wave alternating between a positive and negative

**Fig. 2.1** Longitudinal waves. The expansion and contraction of piezoelectric crystals caused by the application of alternating current to the crystals causes compression and rarefaction of molecules in the body

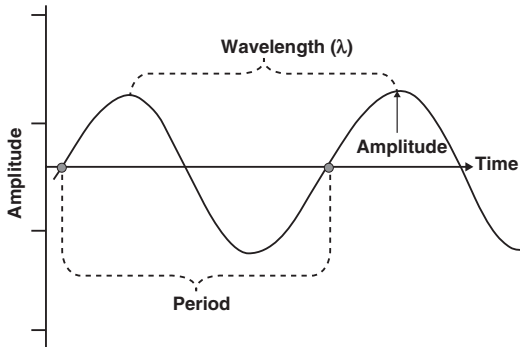
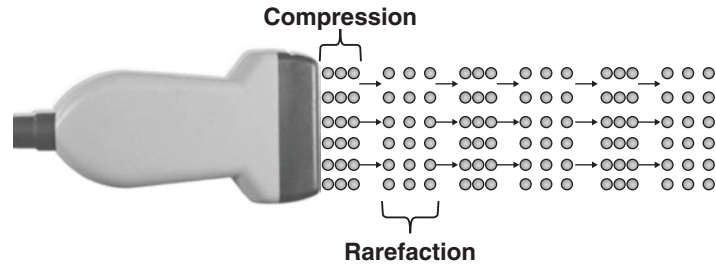


**Fig. 2.2** Characteristics of a sound wave: the amplitude of the wave is a function of the acoustical power used to generate the mechanical compression wave and the medium through which it is transmitted

deflection from the baseline. A **wavelength** is described as the distance between one peak of the wave and the next peak. One complete path traveled by the wave is called a **cycle**. One cycle per second is known as 1 Hz (Hertz). The **amplitude** of a wave is the maximal excursion in the positive or negative direction from the baseline, and the **period** is the time it takes for one complete cycle of the wave (Fig. 2.2).

The velocity with which a sound wave travels through tissue is a product of its frequency and its wavelength. The velocity of sound in tissues is constant. Therefore, as the frequency of the sound wave changes, the wavelength must also change. The average velocity of sound in human tissues is 1540 m/s. Wavelength and frequency vary in an inverse relationship. Velocity equals frequency times wavelength (Fig. 2.3). As the frequency diminishes from 10 to 1 MHz, the wavelength increases from 0.15 to 1.5 mm. This has important consequences for the choice of transducer depending on the indication for imaging.

$$v = f\lambda$$

velocity = frequency x wavelength

**Fig. 2.3** Since the velocity of sound in tissue is a constant, the frequency and wavelength of sound must vary inversely

## Ultrasound Image Generation

The image produced by an ultrasound machine begins with the transducer. **Transducer** comes from the Latin **transducere**, which means to convert. In this case, electrical impulses are converted to mechanical sound waves via the **piezoelectric effect**.

In ultrasound imaging the transducer has a dual function as a sender and a receiver. Sound waves are transmitted into the body where they are at least partially reflected. The piezoelectric effect occurs when alternating current is applied to a crystal containing dipoles [1]. Areas of charge within a piezoelectric element are distributed in patterns which yield a “net” positive and negative orientation. When alternating charge is applied to the two element faces, a relative contraction or elongation of the charged areas occurs resulting in a mechanical expansion and then a contraction of the element. This results in a mechanical wave which is transmitted to the patient (Fig. 2.4).

Reflected mechanical sound waves are received by the transducer and converted back into electrical energy via the piezoelectric effect. The electrical energy is interpreted within the ultrasound instrument to generate an image which is displayed upon the screen.

For most modes of ultrasound, the transducer emits a limited number of wave cycles (usually two to four) called a pulse. The frequency of the two to

**Fig. 2.4** Piezoelectric effect. Areas of “net” charge within a crystal expand or contract when current is applied to the surface, creating a mechanical wave. When the returning wave strikes the crystal, an electrical current is generated

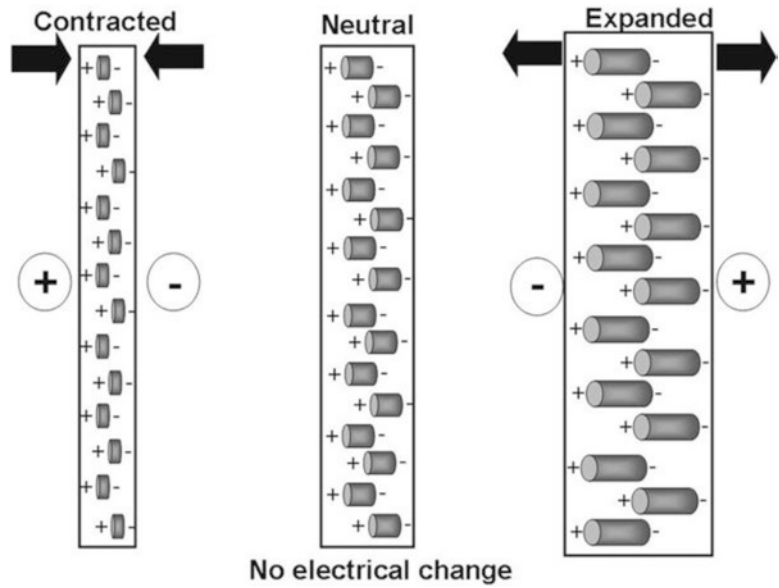
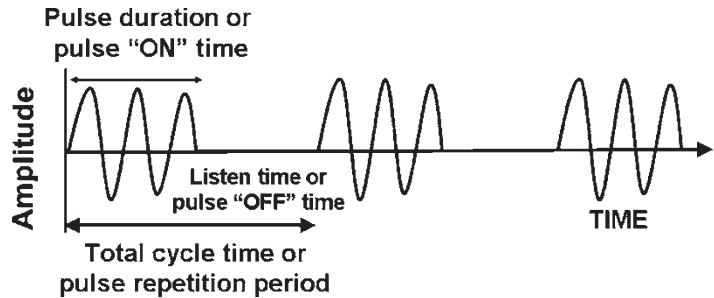


**Fig. 2.5** The pulsed-wave ultrasound mode depends on an emitted pulse of 2–4 wave cycles followed by a period of “silence” as the transducer awaits the return of the emitted pulse



four waves within each cycle is usually in the 2.5–14 MHz range. The transducer is then “silent” as it awaits the return of the reflected waves from within the body (Fig. 2.5). The transducer serves as a receiver more than 99% of the time.

Pulses are sent out at regular intervals usually between 1 and 10 kHz which is known as the **pulse repetition frequency (PRF)**. By timing the pulse from transmission to reception, it is possible to calculate the distance from the transducer to the object reflecting the wave. This is known as **ultrasound ranging** (Fig. 2.6). This sequence is known as **pulsed-wave ultrasound**.

The amplitude of the returning waves determines the brightness of the pixel assigned to the reflector in an ultrasound image. The greater the amplitude of the returning wave, the brighter the pixel assigned. Thus, an ultrasound unit produces an “image” by first causing a transducer to emit a series of ultrasound waves at specific frequencies and intervals

and then interpreting the returning echoes for duration of transit and amplitude. This “image” is rapidly refreshed on a monitor to give the impression of continuous motion. Frame refresh rates are typically 12–30 per second. The sequence of events depicted in Fig. 2.7 is the basis for all “scanned” modes of ultrasound including the familiar gray-scale ultrasound.

### Interaction of Ultrasound with Biological Tissue

As ultrasound waves are transmitted through human tissue, they are altered in a variety of ways including loss of energy, change of direction, and change of frequency. An understanding of these interactions is necessary to maximize image quality and correctly interpret the resultant images.

**Fig. 2.6** Ultrasound ranging depends on assumptions about the average velocity of ultrasound in human tissue to locate reflectors in the ultrasound field. The elapsed time from pulse transmission to reception of the same pulse by the transducer allows for determining the location of a reflector in the ultrasound field

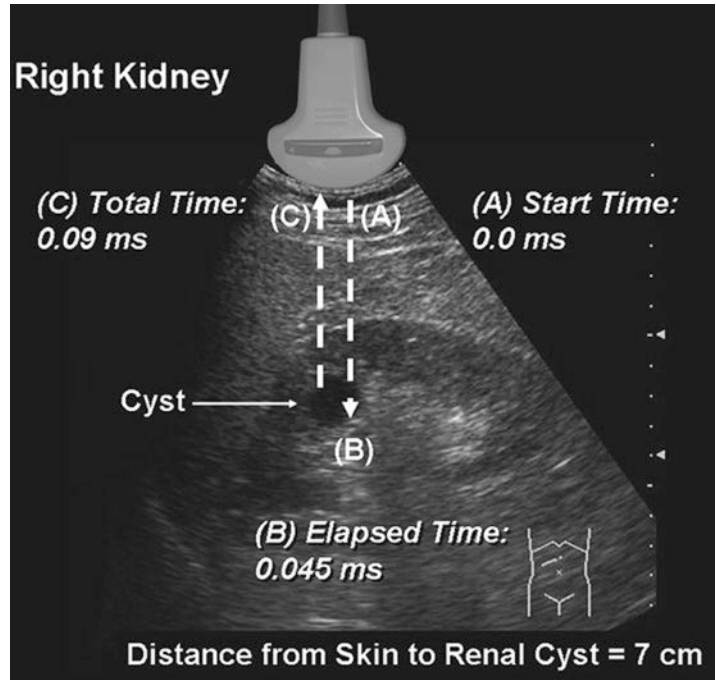
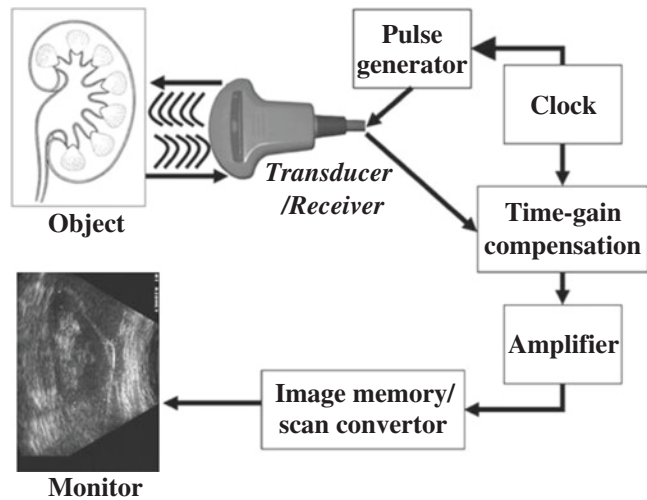


**Fig. 2.7** Schematic depiction of the sequence of image production by an ultrasound device



**Attenuation** refers to a loss of kinetic energy as a sound wave interacts with tissues and fluids within the body [2]. Specific tissues have different potentials for attenuation. For example, water has an attenuation of 0.0 whereas kidney has an attenuation of 1.0 and muscle an attenuation of 3.3. Therefore, sound waves are much more

rapidly attenuated as they pass through muscle than as they pass through water (Fig. 2.8). (Attenuation is measured in dB/cm/MHz.)

The three most important mechanisms of attenuation are absorption, reflection, and scattering. Absorption occurs when the mechanical kinetic energy of a sound wave is converted to

**Fig. 2.8** Attenuation of tissue.) (Adapted from Diagnostic Ultrasound, Third Ed., Vol 1). The attenuation of a tissue is a measure of how the energy of an ultrasound wave is dissipated by that tissue. The higher the attenuation value of a tissue, the more the sound wave is attenuated by passing through that tissue

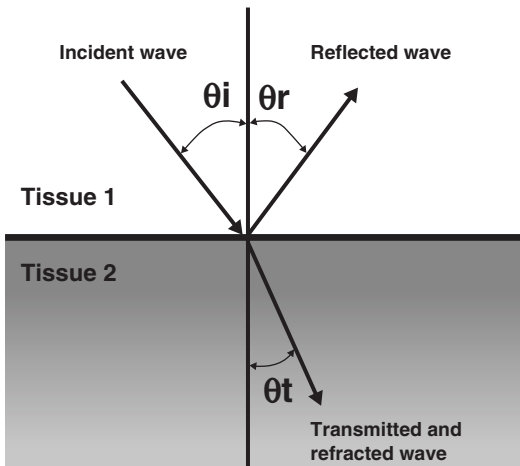
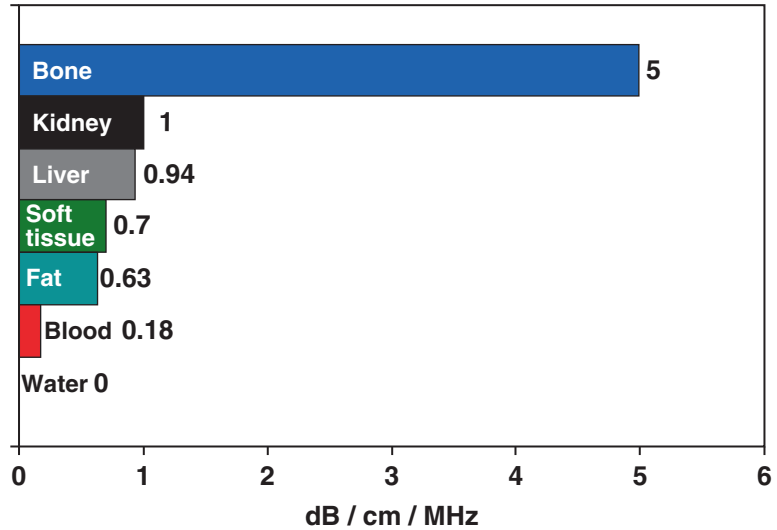


**Fig. 2.9** A wave which strikes the interface between two tissues of differing impedance is usually partially reflected and partially transmitted with refraction. A portion of the wave is reflected at an angle ( $\theta_r$ ) equal to the angle of insonation ( $\theta_i$ ); a portion of the wave is transmitted at a refracted angle ( $\theta_t$ ) into the second tissue

heat within the tissue. Absorption is dependent on the frequency of the sound wave and the characteristics of the attenuating tissue. Higher frequency waves are more rapidly attenuated by absorption than lower frequency waves.

Since sound waves are progressively attenuated with distance traveled, deep structures in the body (e.g., kidney) are more difficult to image. Compensation for loss of acoustic energy by attenuation can be accomplished by the appropriate

use of gain settings (increasing the sensitivity of the transducer to returning sound waves) and selection of a lower frequency.

**Refraction** occurs when a sound wave encounters an interface between two tissues at any angle other than  $90^\circ$ . When the wave strikes the interface at an angle, a portion of the wave is reflected and a portion transmitted into the adjacent media. The direction of the transmitted wave is altered (refracted). This results in a loss of some information because the wave is not completely reflected back to the transducer, but also causes potential errors in registration of object location because of the refraction (change in direction) of the wave. The optimum angle of insonation to minimize attenuation by refraction is  $90^\circ$  (Fig. 2.9).

**Reflection** occurs when sound waves strike an object or an interface between unlike tissues or structures. If the object has a relatively large flat surface, it is called a specular reflector, and sound waves are reflected in a predictable way based on the angle of insonation. If a reflector is small or irregular, it is called a diffuse reflector. Diffuse reflectors produce **scattering** in a pattern which produces interference with waves from adjacent diffuse reflectors. The resulting pattern is called “speckle” and is characteristic of solid organs such as the testes and liver (Fig. 2.10).

When a sound wave travels from one tissue to another, a certain amount of energy is reflected at the interface between the tissues. The percentage

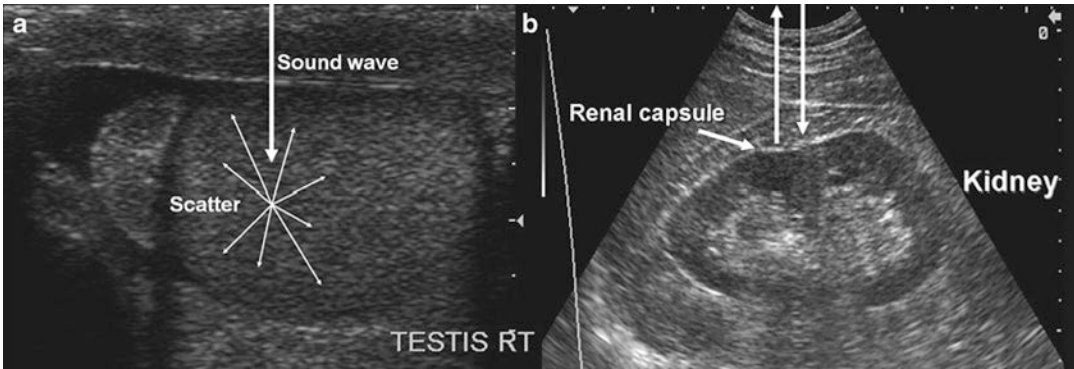


**Fig. 2.10** (a) Demonstrates a diffuse reflector. In this image of the testis, small parenchymal structures scatter sound waves. The pattern of interference resulting from this scattering provides the familiar “speckled” pattern of testicular echo architecture. (b) Demonstrates a specular

reflector. A specular reflector reflects sound waves at an angle equal to the incident angle without producing a pattern of interference caused by scattering. In this image of the kidney, the capsule of the kidney serves as a specular reflector

**Table 2.1** Impedance of tissue

| Tissue                           | Density (kg/m <sup>3</sup> ) | Impedance (Rayles) |
|----------------------------------|------------------------------|--------------------|
| Air and other gases              | 1.2                          | 0.0004             |
| Fat tissue                       | 952                          | 1.38               |
| Water and other clear liquids    | 1000                         | 1.48               |
| Kidney (average of soft tissue)  | 1060                         | 1.63               |
| Liver                            | 1060                         | 1.64               |
| Muscle                           | 1080                         | 1.70               |
| Bone and other calcified objects | 1912                         | 7.8                |

Adapted from Diagnostic Ultrasound, 3rd Ed, Vol. 1  
 Impedance ( $Z$ ) is a product of tissue density ( $\rho$ ) and the velocity of that tissue ( $c$ ). Impedance is defined by the formula:  $Z$  (Rayles) =  $\rho$  (kg/m<sup>3</sup>)  $\times$   $c$  (m/s)

of energy reflected is a function of the difference in the **impedance** of the tissues. Impedance is a property of tissue related to its “stiffness” and the speed at which sound travels through the tissue [3]. If two adjacent tissues have a small difference in tissue impedance, very little energy will be reflected. The impedance difference between kidney (1.63) and liver (1.64) is very small so that if these tissues are immediately adjacent, it may be difficult to distinguish the interface between the two by ultrasound (Table 2.1).

Fat has a sufficient impedance difference from both kidney and liver that the borders of the two organs can be distinguished from the intervening fat (Fig. 2.11).

If the impedance differences between tissues are very high, complete reflection of sound waves may occur, resulting in acoustic shadowing (Fig. 2.12).

## Artifacts

Sound waves are emitted from the transducer with a known amplitude, direction, and frequency. Interactions with tissues in the body result in alterations of these parameters. Returning sound waves are presumed to have undergone alterations according to the expected physical principles such as attenuation with distance and frequency shift based on the velocity and direction of objects they encountered. The timing of the returning echoes is based on the expected velocity of sound in human tissue. When these expectations are not met, it may lead to image representations and measurements which do not reflect actual physical conditions. These misrepresentations are known as “artifacts.” Artifacts, if correctly identified, can be used to aid in diagnosis.

**Increased through transmission** occurs when sound waves pass through tissue with less attenuation than occurs in the surrounding tissues. For example, when sound waves pass through a fluid-filled structure such as a renal cyst, the waves experience relatively little attenuation compared to that experienced in the

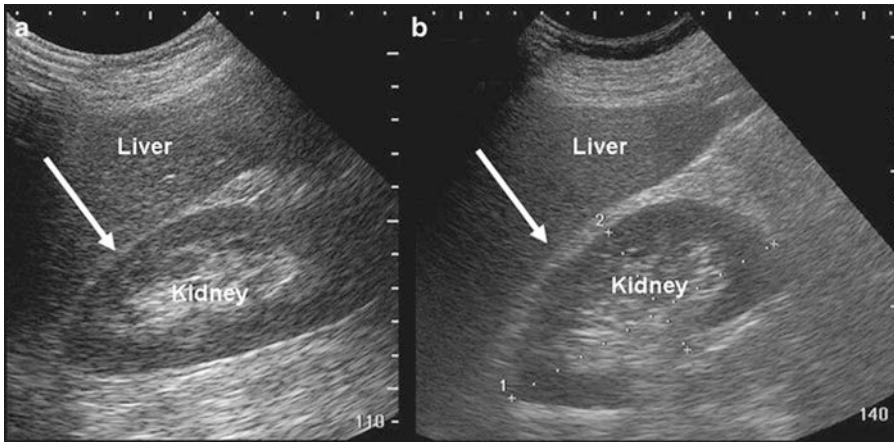


**Fig. 2.11** Image (a) demonstrates that when kidney and liver are directly adjacent to each other, it is difficult to appreciate the boundary (arrow) between the capsules of the kidney and liver. Image (b) demonstrates that when fat

(which has a significantly lower impedance) is interposed, it is far easier to appreciate the boundary between liver capsule (arrow) and fat

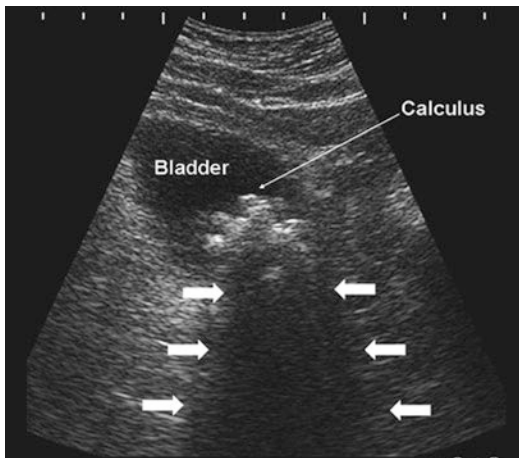


**Fig. 2.12** In the urinary bladder, reflection of sound waves as the result of large impedance differences between urine and the bladder calculus (thin arrow). Acoustic shadowing results from nearly complete reflection of sound waves (arrows)

surrounding renal parenchyma. Thus when the waves reach the posterior wall of the cyst and the renal tissue beyond it, they are more energetic (have greater amplitude) than the adjacent waves. The returning echoes have significantly greater amplitude than waves returning through the renal parenchyma from the same region of the kidney. Therefore, the pixels associated with the region distal to the cyst are assigned a

greater “brightness.” The tissue appears hyperechoic compared to the adjacent renal tissue even though it is histologically identical (Fig. 2.13). This artifact can be overcome by changing the angle of insonation or adjusting the time-gain compensation settings.

**Acoustic shadowing** occurs when there is significant attenuation of sound waves at a tissue interface causing loss of information about other structures distal to that interface. This attenuation may occur on the basis of reflection or absorption, resulting in an “anechoic” or “hypoechoic” shadow. The significant attenuation or loss of the returning echoes from tissues distal to the interface may lead to incorrect conclusions about tissue in that region. For instance, when sound waves strike the interface between testicular tissue and a testicular calcification, there is a large impedance difference and significant attenuation and reflection occur. Information about the region distal to the interface is therefore lost or severely diminished (Fig. 2.14). Thus, in some cases spherical objects may appear as crescentic objects, and it may be difficult to obtain accurate measurements of such three-dimensional objects. Furthermore, fine detail in the region of the acoustic shadow may be obscured. The problems with acoustic shadowing are most appropriately overcome by changing the angle of insonation.

**Fig. 2.13** Increased through transmission with hyperechogenicity (*arrow*) as the result of decreased attenuation by the fluid-filled cyst. This is an example of artifactual misrepresentation of tissue characteristics and must be recognized to avoid incorrect clinical conclusions

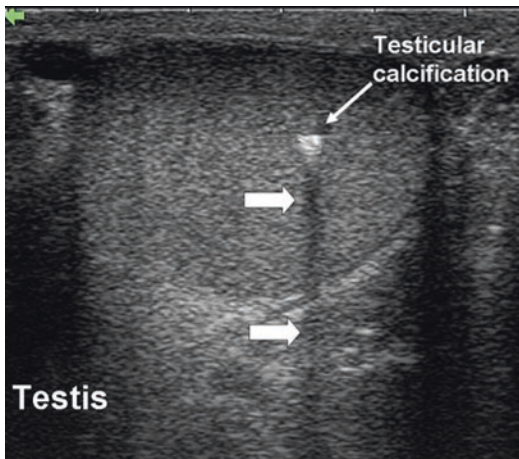
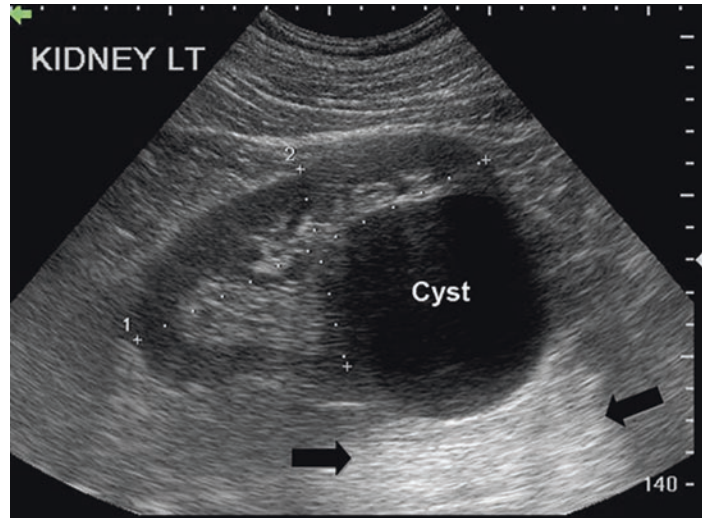


**Fig. 2.14** Acoustic shadowing occurs distal to a calcification in the testis (*large arrows*). Information about testicular parenchymal architecture distal to the area of calcification is lost

**Edging artifact** occurs when sound waves strike a curved surface or an interface at a critical angle. A **critical angle** of insonation is one which results in propagation of the sound wave along the interface without significant reflection of the wave to the transducer. Thus, information distal to the interface is lost or severely diminished. This very common artifact in urology must be recognized and can, at times, be helpful. It is seen in many clinical situations but very commonly seen when imaging the testis. Edging artifacts often occur at the upper and lower pole of the

testis as the sound waves strike the rounded testicular poles at the critical angle. This artifact may help differentiate between the head of the epididymis and the upper pole of the testis. The edging artifact is also prominently seen on transrectal ultrasound, where the two rounded lobes of the prostate come together in the midline. This produces an artifact that appears to arise in the vicinity of the urethra and extend distally. Edging artifact may be seen in any situation where the incident wave strikes an interface at the critical angle (Fig. 2.15). Edging artifact may be overcome by changing the angle of insonation.

A **reverberation artifact** results when an ultrasound wave bounces back and forth (reverberates) between two or more reflective interfaces. When the sound wave strikes a reflector and returns to the transducer, an object is registered at that location. With the second transit of the sound wave, the ultrasound equipment interprets a second object that is twice as far away as the first. There is ongoing attenuation of the sound wave with each successive reverberation resulting in a slightly less intense image displayed on the screen. Therefore, echoes are produced which are spaced at equal intervals from the transducer but are progressively less intense (Fig. 2.16).

The reverberation artifact can also be seen in cases where the incident sound wave strikes a series of smaller reflective objects (such as the